14th International Symposium on Turbulence and Shear Flow Phenomena (TSFP14)
Heidelberg, Germany, July 28-31, 2026

# PASSIVE MANIPULATION OF LOG-LAW CONSTANTS IN TURBULENT CHANNEL FLOW USING RIBLETS AND THERMAL STRATIFICATION

**Hiroya Mamori, Yutaro Koide, Menglei Wang, Takeshi Miyazaki**
Mechanical and Intelligent Systems Engineering
The University of Electro-Communications
1-5-1 Chofugaoka, Chofu-shi, Tokyo, 182-8585, Japan
mamori@uec.ac.jp

**Yusuke Nabae**
Mechanical Systems Engineering
Tokyo Metropolitan University
6-6 Asahigaoka, Hino-shi, Tokyo 191-0065, Japan.
nabae-yusuke@tmu.ac.jp

## ABSTRACT

We investigate the combined effect of riblets and thermal stratification on turbulent channel flow using direct numerical simulations (DNS). The aim is to examine how passive control techniques—riblet structures and buoyancy-induced stratification—can manipulate the logarithmic-law constants $\kappa$ and $B$, thereby reducing skin-friction drag. Three levels of stratification are tested using bulk Richardson numbers $\mathrm{Ri}^+ = -0.1, 0, +0.1$, representing unstable, neutral, and stable conditions. Results show that riblets reduce drag under all stratification conditions. Under stable stratification, turbulence in the channel center is suppressed, and in combination with riblets, a synergistic effect emerges, yielding the highest mean velocity and lowest wall shear stress. The log-law parameters $\kappa$ and $B$ are extracted from the DNS and exhibit changes consistent with theoretical predictions for drag-reducing flows. These values are used in a semi-empirical velocity profile model to predict drag reduction at higher Reynolds numbers. The findings suggest that riblets and buoyancy can jointly realize a passive manipulation of turbulence structure, offering a practical pathway to achieving sustained drag reduction in thermally active flow environments.

## INTRODUCTION

Skin-friction drag reduction in turbulent wall-bounded flows is of great importance for improving energy efficiency in engineering applications. Among passive control techniques, riblets—streamwise-aligned microgrooves on the wall—have been extensively studied for their ability to reduce drag by altering near-wall turbulence structures. Choi et al. (1993) demonstrated that drag reduction occurs when the riblet spacing is smaller than the diameter of near-wall vortices. Subsequent studies explored various riblet geometries, including two-dimensional (2-D) and streamwise-modulated three-dimensional (3-D) designs, with reported drag reductions of up to 11.7% (Sasamori et al., 2014, 2017).

Separately, buoyancy-induced thermal stratification has been shown to significantly affect turbulence: stable stratification suppresses turbulent motions, while unstable stratification enhances them (Garcia-Villalba et al., 2011; Scagliarini et al., 2015). However, the combined effect of riblets and thermal stratification on drag reduction remains largely unexplored.

Recently, Nabae et al. (2026) proposed a theoretical framework showing that the skin-friction drag can be reduced by modifying the logarithmic law in the mean velocity profile, specifically by increasing the integration constant $B$ or decreasing the Kármán constant $\kappa$. While their model predicts sustained drag reduction even at high Reynolds numbers, it assumes idealized or active controls—such as direct damping of spanwise velocity fluctuations—that are difficult to realize in practice.

In this study, we propose a more physically realizable approach: the use of riblets and stable thermal stratification as a passive means to manipulate the logarithmic-law constants $\kappa$ and $B$. Using direct numerical simulations (DNS) of turbulent channel flow with riblets under varying stratification conditions, we investigate how buoyancy modifies the riblet-induced drag reduction mechanism. We also extract $\kappa$ and $B$ from the DNS data and apply a predictive velocity profile model to explore the Reynolds-number dependence of drag reduction. This study provides a practical pathway to implementing logarithmic-law-based drag reduction strategies using passive techniques.

## DIRECT NUMERICAL SIMULATION

DNS are performed for an incompressible turbulent channel flow with riblets mounted on both the upper and lower walls. The flow is driven by a constant mean pressure gradient, and the friction Reynolds number is set to $\mathrm{Re}_\tau = 180$. The governing equations are the incompressible continuity, Navier–Stokes, and energy equations under the Boussinesq approximation, which accounts for buoyancy effects induced by wall temperature differences. The riblets are rectangular in cross-section and modelled using an immersed boundary method (Kim et al., 2001). Their non-dimensional height and spanwise spacing are fixed at $h^+ = 7.5$ and $s^+ = 19.2$, respectively. A total of 30 riblets are uniformly distributed on each wall.

Figure 1(a) shows a schematic of the computational setup, including the riblet geometry and thermal boundary conditions. The rectangular riblets, aligned in the streamwise direction, are designed to interact with near-wall turbulence, while the imposed stable or unstable thermal stratification modifies the turbulence intensity across the channel. The computational domain size is $L_x \times L_y \times L_z = 2\pi \times 2 \times 3.2$, discretized with $N_x \times N_y \times N_z = 128 \times 192 \times 512$ grid points in the streamwise ($x$), wall-normal ($y$), and spanwise ($z$) directions. Periodic boundary conditions are imposed in both the streamwise and spanwise directions, while no-slip boundary conditions are applied at the walls and riblet surfaces.

To induce buoyancy effects, the upper wall is heated, and the lower wall is cooled, generating thermal stratification across the channel. Three cases are considered by varying the Richardson number $\mathrm{Ri}^+$: $\mathrm{Ri}^+ = 0$, neutrally stratified baseline; $\mathrm{Ri}^+ = +0.1$, stable stratification; $\mathrm{Ri}^+ = -0.1$, unstable stratification.

## RESULTS AND DISCUSSION

Figure 2 shows instantaneous vortical structures visualized by $Q$-criterion indicate that riblets push turbulence structures away from the wall in all cases.

To estimate the drag reduction effect, Table 1 summarizes the bulk mean velocities $u_b$ obtained from the DNS for each case. Due to the constant pressure gradient condition, increase of the bulk mean velocity corresponds to skin-friction drag reduction. In the neutral condition ($\mathrm{Ri}^+ = 0$), the introduction of riblets increases $u_b$ from 15.7 to 16.1. Under stable stratification ($\mathrm{Ri}^+ = +0.1$), this trend continues with $u_b$ increasing from 17.0 to 17.3. This confirms that riblets reduce drag not only in neutral conditions but also when buoyancy suppresses turbulence. Interestingly, in the unstable stratification case ($\mathrm{Ri}^+ = -0.1$), the same level of increase is observed (from 15.7 to 16.1), suggesting that the riblet effect remains robust even when turbulence is intensified by buoyancy. These trends in bulk velocity are consistent with the behavior of the log-law constants discussed earlier, where combined riblet and buoyancy effects modify both κ and $B$, leading to enhanced drag reduction.

Figure 3 presents the mean streamwise velocity profiles in wall units for Cases 1-4. Here, the wall-normal coordinate $y$ is adjusted using the virtual origin $y_0$ proposed by Endrikat et al. (2021). Riblets increase the centerline velocity under both neutral and stable conditions, indicating reduced skin friction. The stable + riblet case exhibits the highest $u^+$, suggesting a synergistic effect between buoyancy and wall structures. Additionally, velocities near the wall decrease due to the riblets.

Figure 4 shows the diagnostic function $1/\kappa = y^+(\mathrm{d}\, u^+/\mathrm{d}y^+)$, which reflects the local slope of the logarithmic region. The $\kappa$ was determined by averaging the diagnostic function within the logarithmic region. Subsequently, $B$ is obtained using the least-squares method. The calculated values of $\kappa$ and $B$ are summarized in Table 2. Compared to Case 1, Case 2 shows almost no change in the Kármán constant, while the additive constant exhibits an increase. In Case 3, both a larger slope (smaller $\kappa$) and an upward shift in the logarithmic layer are evident, indicating that both the Kármán constant and the additive constant are modified by the combined control. These changes in the log-law parameters align with the theoretical predictions by Nabae et al. (2026), who showed that decreasing $\kappa$ and increasing $B$ leads to sustained drag reduction at high Reynolds numbers.

To estimate the potential of drag reduction at higher Reynolds numbers, the extracted values of $\kappa$ and $B$ are applied to a velocity profile model based on the Reynolds–Tiederman framework. The predicted drag reduction rate $R_D$ as a function of $\mathrm{Re}_\tau$ up to $10^3$ is shown in Fig. 5 (top). The markers indicate DNS results, while the predicted results are shown as lines. In Case 2, the two results show excellent agreement; however, for Cases 3 and 4, they do not coincide. Figure 5(bottom) presents the drag reduction rates for the range of $\mathrm{Re}_\tau = 180$ to $10^4$. For Case 2, the model predicts that the drag reduction rate initially increases with the Reynolds number and subsequently undergoes a gradual decrease. We attribute this trend to the fact that the effective flow-narrowing effect caused by the riblets becomes relatively smaller as the Reynolds number increases, leading to a state where the effect of the increased integration constant becomes dominant. Regarding Cases 3 and 4, we expect the drag reduction rate to gradually increase as the Reynolds number rises.

This result suggests that stable stratification enhances the effect of riblets not only at low Reynolds numbers but also in extrapolated high-Re regimes, validating the feasibility of passive control strategies that modify the logarithmic law through physically realizable means.

## CONCLUSION

We have performed direct numerical simulations of turbulent channel flow with riblets under various thermal stratification conditions to evaluate the combined effects of passive wall geometry and buoyancy on skin-friction drag reduction. Key findings include:

- Riblets reduce drag in all stratification regimes, with further enhancement observed under stable stratification.
- Unstable stratification increases turbulence intensity but does not diminish the riblet effect.
- The log-law constants κ and $B$ are altered by the combined control, aligning with theoretical predictions (Nabae et al., 2026).
- In the case with riblets only, the predicted drag reduction rate $R_D$ agreed with the DNS results; the model predicts that $R_D$ initially increases and then gradually decreases as the Reynolds number rises. For the cases with stable stratification, $R_D$ is predicted to gradually increase with the Reynolds number.
- For the case with riblets only, the prediction of the drag reduction rate by Nabae et al. (2026) is considered to hold true.

These results demonstrate a feasible and scalable approach to passive drag reduction by leveraging wall geometry and thermal gradients. Future work will address the Reynolds-number dependence of κ and $B$ and extend the present model to higher Reynolds number regimes relevant to industrial applications.

Table 1. Bulk mean velocity obtained from DNS

| | Stratification | Riblet | $u_b^+$ |
|---|---|---|---|
| Case 1 | Ri = 0 (Neutral) | Without | 15.7 |
| Case 2 | Ri = 0 (Neutral) | With | 16.1 |
| Case 3 | Ri = 0.1 (Stable) | Without | 17.0 |
| Case 4 | Ri = 0.1 (Stable) | With | 17.3 |
| Case 5 | Ri = -0.1 (Unstable) | Without | 15.7 |
| Case 6 | Ri = -0.1 (Unstable) | With | 16.1 |

Table 2. Kármán constant and Integral constant from DNS

| | κ | $B$ |
|---|---|---|
| Case 1 | 0.355 | 4.27 |
| Case 2 | 0.354 | 5.17 |
| Case 3 | 0.255 | 0.63 |
| Case 4 | 0.253 | 1.37 |

## REFERENCES

Choi, H., Moin, P., and Kim, J., "Direct numerical simulation of turbulent flow over riblets", J. Fluid Mech., 255 (1993), 503–539.

Endrikat, S., Modesti, D., García-Mayoral, R., Hutchins, N., and Chung, D., "Reorganisation of turbulence by large and spanwise-varying riblets", J. Fluid Mech., 941 (2022), A17.

Garcia-Villalba, M., and Del Álamo, J.C., "Turbulence modification by stable stratification in channel flow", Phys. Fluids, 23 (2011), 045104.

Kim, J., Kim, D., and Choi, H., "An immersed boundary finite-volume method for simulations of flow in complex geometries", J. Comput. Phys. 171, (2001), 132–150.

Nabae, Y. Mamori, H., Gotoda, H., and Fukagata, K., Effect of manipulating logarithmic law on friction drag reduction in a turbulent channel flow 14th International Symposium on Turbulence and Shear Flow Phenomena (TSFP14), 114, July 28–31, 2026, Heidelberg, Germany.

Sasamori, M., Iihama, O., Mamori, H. Iwamoto, K., and Murata, A., "Parametric study on a sinusoidal riblet for drag reduction by direct numerical simulation." Flow Turbul. Combust. 99, (2017), 47–69.

Sasamori, M., Mamori, H., Iwamoto, K., and Murata, A., "Experimental study on drag reduction effect due to sinusoidal riblets channel flow," Exp. Fluids. 55 (2014), 1828.

Scagliarini, A., Einarsson, H., Gylfason, Á., and Toschi, F., "Law of the wall in unstably stratified turbulent channel flow", J. Fluid Mech. 781 (2015), R5.

Reynolds, W. C. and Tiederman, W. G., "Stability of turbulent channel flow, with application to Malkus's theory", J. Fluid Mech. 27, 1967, 253–272.

## ACKNOWLEDGMENTS

This work was supported through JSPS KAKENHI (Grant Number 24K07300) and by the JKA Foundation through the KEIRIN/Auto Race funding program.

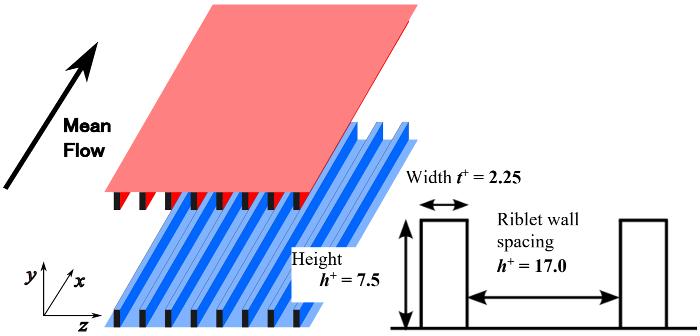


Figure 1. Schematic of the channel flow with the riblet surfaces.

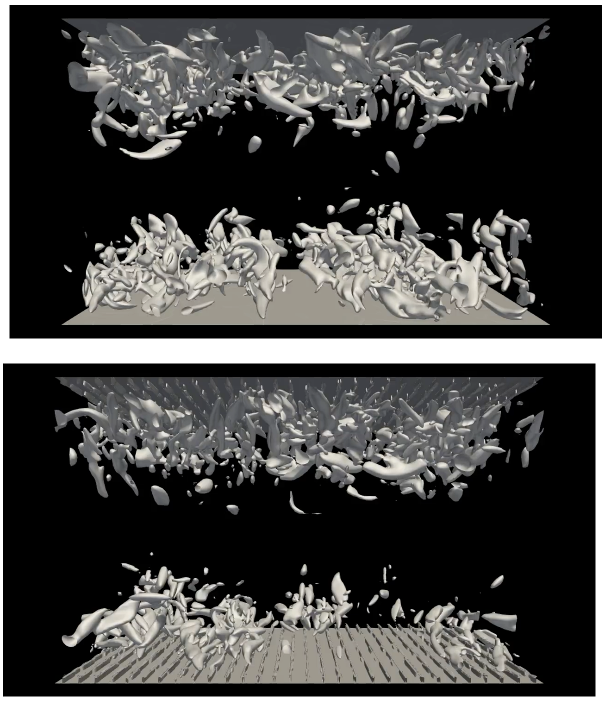

Figure 2. Visualization of vortical structure: top, Ri =0 and w/o riblet; bottom, Ri = 0.1w/ riblet.

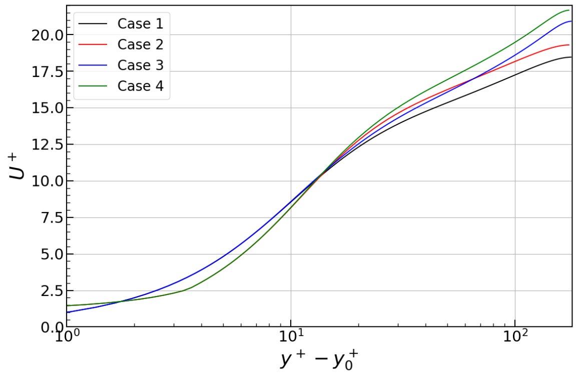


Figure 3. Mean velocity profile from DNS.

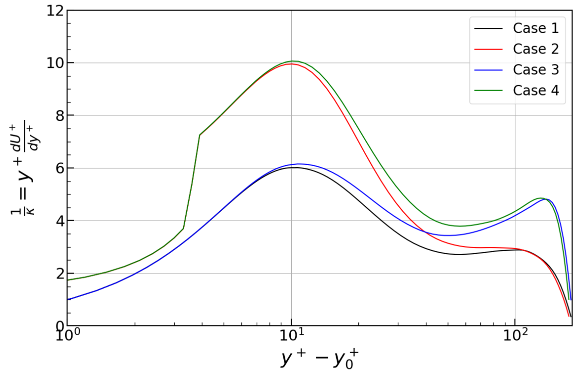


Figure 4. Kármán constant from DNS.

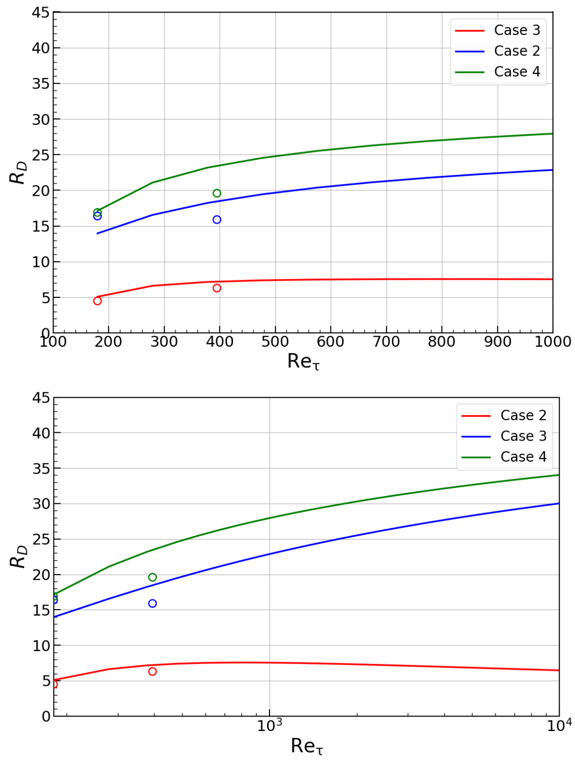


Figure 5. Prediction of drag reduction rate as a function of Reynolds number.